SLAC-PUB-8279
June 1999

Saturation of the Coherent Beam-Beam Instability *

S. Heifets

Stanford Linear Accelerator Center, Stanford University, Stanford, CA 94309, USA

1 Abstract

The non-linear regime of the beam-beam instability for flat beams is considered. It is shown that the exponential growth of the linear approximation saturates what leads to a finite growth of transverse emittance. Mode interaction and excitation of linearly stable modes is studied.

2 Introduction

The beam blow-up due to the beam-beam interaction is one of the main factors limiting luminosity and life time in circular colliders. Effect is well known and has been studied both theoretically, numerically, and experimentally. In particular, the coherent beam-beam instability was studied and its importance was emphasized, see for example [1].

This note considers two mechanisms of beam-beam blow-up: one is due to harmonics of periodic beam-beam kicks generated by rigid bunch of the opposite beam, and another is due to saturation of the linearly unstable beam-beam coherent modes. The last process is similar to the microwave instability. The process can be described as excitation of unstable modes which, in their turn, modify the bunch distribution to a new steady-state equilibrium. Hopefully, these mechanisms may explain emittance blow-up in the flip-flop regime.

Mode coupling and excitation of linearly stable modes is also discussed.

A flat beam is assumed with parameters of the PEP-II B-factory [2]. For the sake of compliteness, the basic formulas are re-derived.

*Supported by Department of Energy contract DE–AC03–76SF00515.

3 Basic Kinematics and Notations

The steady-state can be described by the Hamiltonian averaged over revolution period. Below the threshold of coherent instability, action-angle variables I, α can be chosen to make the steady-state (Haissinski) Hamiltonian $H_H(I)$ independent of α, for details see Appendix 1. In the lowest order in the beam-beam parameter, we can neglect all anharmonic terms in a particle motion. In this approximation, $y = \Delta y_0 + w\sqrt{2I}\cos\alpha$, where Δy_0 is distance between beam centroids (vertical beam offset), $w = \sqrt{\beta_y}$, and β_y is vertical beta-function.

The steady-state normalized distribution function $\rho_H(I)$ of a beam is also depend only on I and, approximately, is $\rho_H(I) = \frac{1}{2\pi\epsilon}e^{-I/\epsilon}$ where $\epsilon = \sigma^2/\beta$ is transverse beam emittance. Distribution ρ_H is normalized, $2\pi\int dI\,\rho_H(I) = 1$.

The full distribution function $\rho(I, \alpha, \phi)$ is the sum of azimuthal harmonics. For the first bunch,

$$\rho_1(I, \alpha, \phi) = \rho_H^{(1)}(I) + \sum_{n=-\infty}^{\infty} \rho_n^{(1)}(I, \phi)e^{in\alpha}, \quad \rho_{-n} = \rho_n^{c.c.} \tag{1}$$

The average effect of the beam-beam interaction depends on the beam-beam parameter ξ^{BB}. For the first beam,

$$\xi_1^{BB} = \frac{N_b^{(2)} r_0 \beta_{1,y}^*}{2\pi\gamma_1\sigma_{2,y}(\sigma_{2,x} + \sigma_{2y})}. \tag{2}$$

ξ_2^{BB} for the second beam can be obtained interchanging indexes.

Beam-beam parameter is, usually, small, $\xi < 0.05$. Hence, the steady-state effect of the beam-beam force leads only to small transverse potential well distortion and can not explain the beam blow-up. This also allows us to use Gaussian distribution as the zero-order bunch distribution function.

The Hamiltonian of the system is the sum of Hamiltonians of two beams

$$H = H_1(I_1, \alpha_1, \phi) + H_2(I_2, \alpha_2, \phi), \tag{3}$$

each one of them depends on the distribution function of another bunch. The Hamiltonian in the angle-action variables takes into account all azimuthal harmonics of the distribution function ρ_k,

$$H_1(I, \alpha, \phi) = H_H^{(1)} + 2\pi\Lambda_1 \sum_{n,m\neq 0} e^{i(n\alpha - m\phi)} \int dI'[S_{n0}(I, I', \Delta y)\rho_H^{(2)}(I') + \sum_k S_{n,k}\rho_k^{(2)}(I')] \tag{4}$$

$$+2\pi\Lambda_1 \sum_n e^{in\alpha} \sum_k \int dI' S_{n,k}(I, I', \Delta y)\rho_k^{(2)}(I', \phi). \tag{5}$$

Here, the parameter

$$\Lambda_1 = \frac{2N_b^{(2)} r_0}{2\pi\gamma_1}, \tag{6}$$

and the function $S_{n,l}$ for a flat beam can be written (neglecting anharmonic corrections to the trajectory and factor $e^{-(\Delta x)^2/2\Sigma_x^2}$) as

$$S_{n,l}(I,I',\Delta y_0) = -\int_0^\infty \frac{d\xi}{\xi}\mathrm{Erfc}[\xi]\{\cos[(n-l)\frac{\pi}{2}+\frac{\Delta y_0\sqrt{2}}{\Sigma_x}\xi]J_n(\frac{2w_1\sqrt{I}}{\Sigma_x}\xi)J_l(\frac{2w_2\sqrt{I'}}{\Sigma_x}\xi)-1\}, \tag{7}$$

where $\mathrm{Erfc}(\xi) = e^{\xi^2}[1-\mathrm{Erf}(\xi)]$, $\mathrm{Erf}(\xi)$ is error function. For a flat beam the main contribution is given by large $\xi >> 1$. In this case, $\mathrm{Erfc}(\xi) \simeq 1/(\xi\sqrt{\pi})$.

For more details, see Appendices 1,2.

The steady-state Hamiltonian is defined by

$$H_H^{(1)}(I) = Q_1 I - \frac{\Lambda_1\sigma_{2y}}{\sqrt{\pi}\Sigma_x}\int_0^\infty \frac{dx}{x^2}J_0(\frac{2w_1\sqrt{I}}{\sigma_{2,y}}x)\cos[\frac{\Delta y_0\sqrt{2}}{\sigma_{2,y}}x]e^{-x^2}. \tag{8}$$

Eq. (8) defines frequency $\omega_1(I) = dH_H/dI = Q_1 + \Delta Q_1(I)$, where, see Fig. 1,

$$\Delta Q_1(I) = \frac{\Lambda_1 w_1}{\Sigma_x\sqrt{\pi I}}\int_0^\infty \frac{dx}{x}J_1(\frac{2w_1\sqrt{I}}{\sigma_2}x)\cos(\frac{\Delta y_0\sqrt{2}}{\sigma_2}x)e^{-x^2}. \tag{9}$$

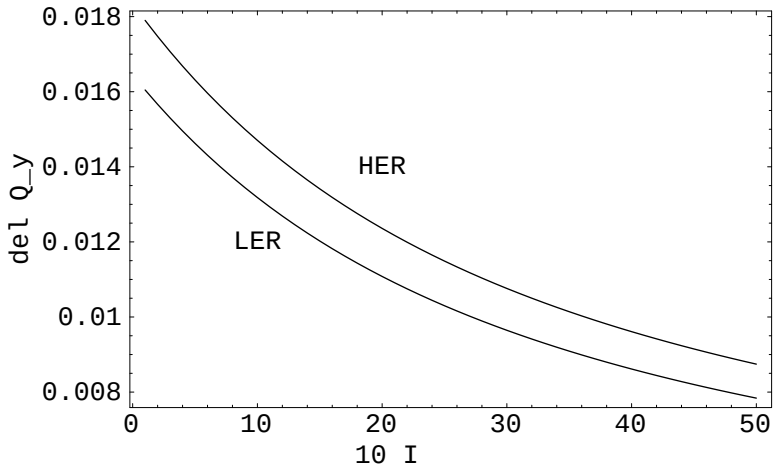

Figure 1: Dependence of the tune shift $\Delta Q(I)$ on I. The action I is in units of the rms emittance ϵ.

Hamiltonian H_2 for the second beam can be obtained by interchanging indexes 1 and 2, and substituting $S_{k,n}(I',I,\Delta y)$ for $S_{n,k}(I,I',\Delta y)$.

4 Effect of the Nonlinear Resonances

If non-zero components ρ_k can be neglected, the simplified Hamiltonian is

$$H_1(I,\alpha,\phi) = H_H^{(1)} + \sum_n\sum_{m\neq 0} U_n(I)e^{i(n\alpha-m\phi)}, \tag{10}$$

where the functions

$$U_n(I) = 2\pi\Lambda_1 \int dI' S_{n0}(I, I', \Delta y)\rho_H^{(2)}(I') \tag{11}$$

are defined (cf. Eq. (71) in Appendix 2) by:

$$U_n(I) = -\frac{\Lambda_1\sigma_{2,y}}{\Sigma_x\sqrt{\pi}}\int_0^\infty \frac{dx}{x^2}e^{-x^2}J_n[2x\frac{\sigma_{1y}}{\sigma_{2y}}\sqrt{\frac{I}{\epsilon_1}}]\cos[\frac{n\pi}{2} + \frac{\Delta y_0}{\sigma_{2y}}\sqrt{2}x]. \tag{12}$$

For zero offsets $U_n \neq 0$ only for even $n = 2k$. In this case, U_{2k} is given in terms of the degenerate hypergeometric function,

$$U_{2k} = (-1)^{k+1}\frac{\Lambda_1\sigma_{2y}}{2\Sigma_x\sqrt{\pi}}\frac{\Gamma(k-1/2)}{\Gamma(2k+1)}(\frac{\sigma_{y1}}{\sigma_{y2}})^{2k}(\frac{I}{\epsilon_1})^k F[k-1/2, 2k+1, -(\frac{\sigma_{y1}}{\sigma_{y2}})^2\frac{I}{\epsilon_1}]. \tag{13}$$

Hamiltonian Eq. (10) is the Hamiltonian of a nonlinear oscillator with frequency $\omega_1(I) = dH_H(I)/dI$ in the external periodic potential.

The perturbation due to beam-beam kicks is small, of the order of Λ, except I near the resonances $\omega_1(I_R) = m/n$. Particles with amplitudes $I \simeq I_R$ are trapped in a separatrix and the modulation of their amplitudes is of the order of the size of the separatrix, $\Delta I = 2\sqrt{2U_{nm}(I_R)/\omega_1'(I_R)}$, where $\omega_1'(I) = d^2H_1(I)/dI^2$. Usually, ω' due to lattice non-linearities is small. In this case, both terms $U_{n,m}$ and ω' are proportional to Λ and dependence of the width ΔI on current arizes only through the dependence of the shape ρ_H on current. If ΔI is comparable to the vertical emittance ϵ_1, the rms σ_y defining $U_{n,m}$ has to be understood as a self-consistent parameter.

For small I and zero offsets, the widths of even resonances $n = 2k$ are

$$(\Delta I)_{2k} = \frac{4\sqrt{2}\epsilon}{\pi^{1/4}2^k\sqrt{(k-1/2)k!}}(\frac{I}{\epsilon})^{k/2}\ (\frac{\sigma_{y1}}{\sigma_{y2}})^{k-2}. \tag{14}$$

Fig. 2 shows ΔI for several resonances.

Particles trapped in the resonance separatrix change the distribution function [3]. For small separatrices

$$\rho(I) = \frac{1}{Z}e^{-\frac{1}{T}[H(I)\mp\omega(I_R)\Delta I\Psi(0)]}, \tag{15}$$

where $H(I) \simeq Q_y I$, $T = Q_y\epsilon_y$, $\Psi(0) = 0.69$, and plus (minus) sign corresponds to amplitudes above (below) resonance amplitude I_R.

Resonance changes unperturbed rms $< I/\epsilon_y >= 1$ to

$$< I/\epsilon_y >= 1 + 2\frac{(\Delta I)_{2k}}{\epsilon_y}\Psi(0)(\frac{I_R}{\epsilon_y})\ e^{-\frac{I_R}{\epsilon_y}}, \tag{16}$$

for small $(\Delta I)_n/\epsilon$.

Emittance distortion is small for higher order resonances, see Fig. 3.

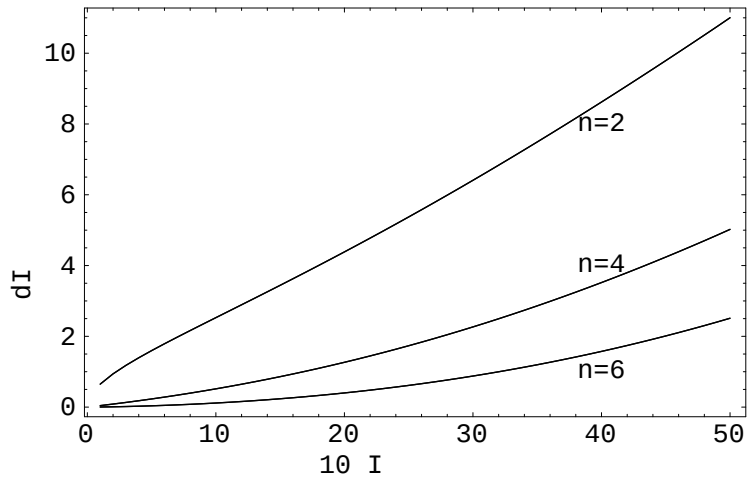

Figure 2: The resonance width $\Delta I/\epsilon$ for resonances $n\omega(I_R) = integer$ vs. I_R (I_R is in units of ϵ.

5 The Fokker-Plank Equation

In this section we assume that the weak-strong resonances $\omega = n/m$ considered in the previous section are avoided by a proper choice of the working point in the tune diagram. This allows us to drop term proportional to ρ_H. Perturbation in this case is produced by the azimuthal harmonics of the distribution function,

$$H_1(I,\alpha,\phi) = H_H^{(1)} + 2\pi\Lambda_1 \sum_{n,m=-\infty}^{\infty} e^{i(n\alpha - m\phi)} \int dI' \sum_k S_{n,k}\rho_k^{(2)}(I',\phi) \qquad (17)$$

Term $k = 0$ describes dynamic variation of the distribution function and plays crucial role in the following considerations.

Let us start with the Fokker-Plank equation in y, q, ϕ variables:

$$\frac{\partial\rho}{\partial\phi} + \{H,\rho\}_{q,y} = Q_y\beta_y\frac{\partial}{\partial q}[D\frac{\partial\rho}{\partial q} + \gamma_0 q\rho]. \qquad (18)$$

Here the diffusion D is due to coupling to SR fluctuations in horizontal plane and γ_0 is vertical damping. Damping gives $< q > \propto e^{-\gamma_0 s}$, diffusion causes rms growth $< q^2 >= 2Ds$, and their ratio defines equilibrium temperature $T =< q^2 >= D/\gamma_0 = \epsilon_y/\beta_y$, related to vertical emittance ϵ and vertical rms $< y^2 >= \sigma_y^2$.

The rhs of Eq. (18) averaged over α can be written in I, α variables as

$$R_k^{(1)} = \gamma_0\frac{\partial}{\partial I}\{\epsilon^{(1)}I\frac{\partial\rho_k^{(1)}}{\partial I} + I\rho_k^{(1)}\} - \gamma_0\frac{k^2\epsilon_1}{4I}\rho_k^{(1)}. \qquad (19)$$

Here we have neglected betatron resonances $Q_y = n/m$ considered above, replaced $Q_y\beta_y$ by its average value over one turn $\int(d\phi/2\pi)Q_y\beta_y = R$, and introduced dimen-

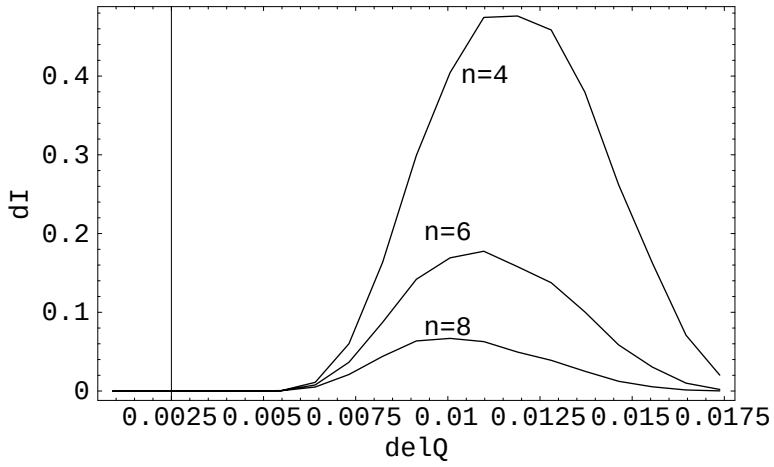

Figure 3: Distortion of the beam emittance $\Delta I/\epsilon$ due to $n = 2k$-order resonance vs detuning.

sionless $\gamma_0 = 1/(\omega_0 \tau_{SR})$, where $\omega_0/(2\pi)$ is revolution frequency and τ_{SR} is radiation damping time.

The Fokker-Plank equation for azimuthal harmonics $\rho_k(I,\phi)$ takes form

$$\frac{\partial \rho_k^{(1)}}{\partial \phi} + ik\omega_1(I)\rho_k^{(1)} + i\Lambda_1 \sum_{m,n,l} (k-l)\rho_{k-l}^{(1)} e^{im\phi} \int dI' d\alpha' \rho_n^{(2)}(I') \frac{\partial S_{ln}(I,I')}{\partial I} - \qquad (20)$$

$$-i\Lambda_1 \sum_{m,n,l} l \frac{\partial(\rho_H \delta_{k,l} + \rho_{k-l}^{(1)})}{dI} e^{im\phi} \int dI' d\alpha' \rho_n^{(2)}(I') S_{ln}(I,I',\Delta y_0) = R_k^{(1)}. \qquad (21)$$

Harmonics ρ_0 satisfies the following equation:

$$\frac{\partial \rho_0^{(1)}}{\partial \phi} - i\Lambda_1 \frac{\partial}{\partial I} \sum_{m,n,l} l[\rho_l^{(1)}]^{cc} e^{im\phi} \int dI' d\alpha' \rho_m^{(2)}(I') S_{lm}(I,I',\Delta y_0) = R_0^{(1)}. \qquad (22)$$

Equation for the second beam can be obtained replacing index $1 \to 2$ and $S_{nl}(I,I',\Delta y_0)$ by $S_{l,n}(I',I,\Delta y_0)$ because $S_{ln}(I,I',-\Delta y_0) = S_{nl}(I',I,\Delta y_0)$.

For small coherent tune shifts $\Delta Q << 1$, dependence on ϕ of azimuthal harmonics is given mainly by the factor $e^{-ikQ_y\phi}$.

Generally, there is a dense net of resonances in the plane Q_{y1}, Q_{y2}, see Fig. 4. Each resonance line is represented by a line with a width defined by the tune dependence on amplitude. The width of the lane is of the order of the beam-beam parameter and increases with the bunch current. Eventually, resonances overlap and the motion become stochastic.

Let us consider bunch current near but above the threshold of the coherent beam-beam instability. In this case, the tune spread with amplitude within the

bunch distribution can be smaller than the distance to the low order resonances. Higher order resonances are suppressed by the synchrotron damping. For electron machines suffice to consider resonances of the order $|n_0| + |m_0| <= 4$. In this case, we can consider isolated resonances and assume that beam dynamics is defined by the resonance $(n_0,\ l_0)$ with the smallest detuning $\Delta m \equiv n_0 Q_{1,y} - l_0 Q_{2,y} - m_0$.

This allows us to average fast oscillating terms and retain only equations for harmonics $\rho^{(1)}_{n0}$ and $\rho^{(2)}_{l0}$.

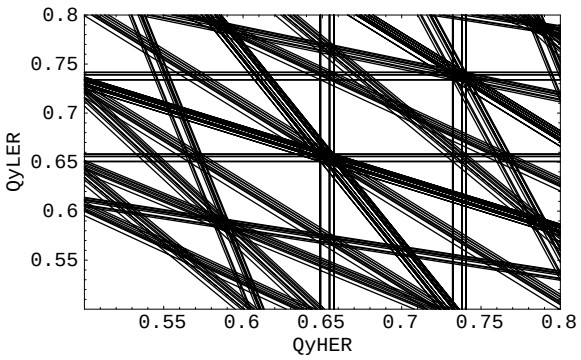

Figure 4: Coherent resonances $nQ_{1y} - lQ_{2y}$, $|n, l| <= 4$. Three lines with $I/\epsilon = 0, 2, 4$ are drawn for each resonance to illustrate dependence $Q(I)$.

Let us introduce slow functions $f^{(1)}_{n0}$ and $f^{(2)}_{l0}$

$$\rho^{(1)}_{n0} = f_1 e^{-in_0 Q_1 \phi + i\Delta m/2\phi}, \quad \rho^{(2)}_{l0} = f_2 e^{-il_0 Q_2 \phi - i\Delta m/2\phi}. \tag{23}$$

In the linear approximation, these functions satisfy the coupled system of equations

$$\frac{\partial f_1}{\partial \phi} + i[n_0(\omega_1(I) - Q_1) + \frac{\Delta m}{2}]f_1 - i\Lambda_1 n_0 \frac{\partial \rho^{(1)}_H}{\partial I} \int dI' d\alpha' f_2(I') S_{n0,l0}(I, I') = 0, \tag{24}$$

$$\frac{\partial f_2}{\partial \phi} + i[l_0(\omega_2(I) - Q_2) - \frac{\Delta m}{2}]f_2 - i\Lambda_2 l_0 \frac{\partial \rho^{(2)}_H}{\partial I} \int dI' d\alpha' f_1(I') S_{n0,l0}(I', I) = 0. \tag{25}$$

The system has a solution in the form

$$f_1(I, \phi) = \sqrt{|\Lambda_1 n_0 \frac{\partial \rho^{(1)}_H}{\partial I}|}\, X e^{-i\nu\phi}, \quad f_2(I, \phi) = \sqrt{|\Lambda_2 l_0 \frac{\partial \rho^{(2)}_H}{\partial I}|}\, Y e^{-i\nu\phi}. \tag{26}$$

The vectors (X, Y) are eigen-vectors of the matrix

$$\begin{pmatrix} (n_0 \Delta Q_1 + \Delta m/2)\delta(I - I') & -sign(n_0) K(I, I') \\ -sign(l_0) K^T(I, I') & (l_0 \Delta Q_2 - \Delta m/2)\delta(I - I') \end{pmatrix}.$$

Here $K(I,I') = 2\pi\sqrt{|\Lambda_1\Lambda_2 n_0 l_0 \frac{\partial\rho^{(1)}}{\partial I}\frac{\partial\rho^{(2)}}{\partial I}|}$, and K^T is transposed matrix, $K^T(I,I') = K(I',I)$. Because this matrix is real and symmetric, the eigen-values ν are real and the system is stable provided $n_0 l_0 > 0$. Hence, instability is possible only if $n_0 l_0 < 0$, i.e. for the sum resonances.

It should be mentioned though that this conclusion is derived from the explicit form of $S_{n,l}(I,I')$ which was calculated by neglecting all anharmonic terms in the trajectory $Y(I,\alpha,\phi)$. It is well known that for microwave instability exactly these terms are responsible for onset of instability. However, for the beam-beam interaction at the sum resonances these terms give only small corrections although they may be important for the difference resonances.

It is worth noting that if $n - l = odd$, $S_{nl} \neq 0$ only for nonzero offsets Δy_0.

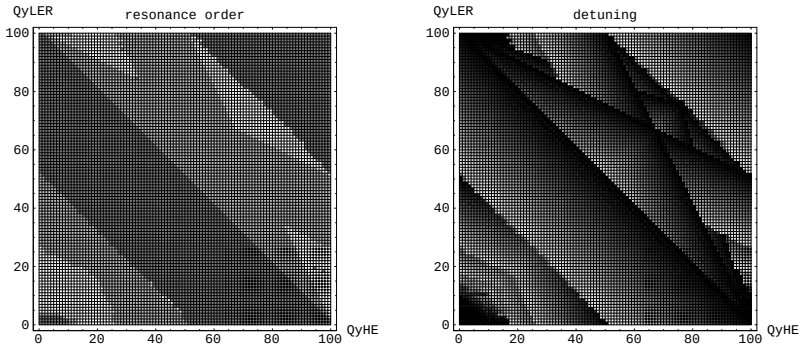

Figure 5: Figure on the left shows the order of the lowest resonance for a working point in the unit square of the vertical plane Q_{y1},Q_{y2}. Light spots corresponds to less dangerous resonances of higher order. Light (dark) spots in the right figure correspond to large (small) detuning from the strongest resonances shown in the left figure.

Effect of a resonance on beam dynamics depends on the resonance order $|n_0| + |l_0|$ and the detuning $\Delta m = n_0 Q_{1,y} - l_0 Q_{2y}$. Fig.5 shows the order of the closest resonance in the vertical tune plane $Q_{y,1},\ Q_{2,y}$ of unit size. For a working point $Q_{y,1},\ Q_{2,y}$ there are several resonances of the same order. Fig. 5 on the right depicts the minimum detuning from the working point found for the resonances of the same order. Only the sum resonances $n_0 l_0 < 0$ which are above and to the right from the working point are taken into account. In this case, the tune is shifted toward the resonance due to finite amplitudes of betatron oscillations. The most dangerous working points (low order, small detuning) are in the darkest areas of the diagrams.

6 The Linear Approximation

In the linear approximation, let us expand slow functions in Eq. (23) in eigen-vectors $V_\nu = \{Y_\nu, X_\nu\}$,

$$f_1(I,\phi) = \frac{\partial \rho_H^{(1)}}{\partial I} \sum_\nu A_\nu Y_\nu e^{-i\nu\phi}, \quad f_2(I,\phi) = \frac{\partial \rho_H^{(2)}}{\partial I} \sum_\nu A_\nu X_\nu e^{-i\nu\phi}. \tag{27}$$

Vector $V_\nu(I) = (X_\nu, Y_\nu)$ is eigen-vector of the matrix M, $\int M(I,I')V_\nu(I')dI' = -\nu V_\nu(I)$,

$$M = \begin{pmatrix} (-l_0\Delta Q_2 + \Delta m/2)\delta(I-I') & M_2 \\ M_1 & (-n_0\Delta Q_1 - \Delta m/2)\delta(I-I') \end{pmatrix},$$

where

$$M_1(I,I') = 2\pi\Lambda_1 n_0 \frac{d\rho_H^{(2)}(I')}{dI'} S_{n0,l0}(I,I') \tag{28}$$

$$M_2(I,I') = 2\pi\Lambda_2 l_0 \frac{d\rho_H^{(1)}(I')}{dI'} S_{n0,l0}(I',I). \tag{29}$$

The norm $\int dI \hat{V}_\mu V_\nu = \delta_{\nu,\mu}$, where $\hat{V}_\mu$ are eigen-vectors of the transposed matrix M^T.

The nominal parameters of the B-factory:

$N^0_{HER} = 1.74\ 10^{10}$; $N^0_{LER} = 5.617\ 10^{10}$; $\Sigma_x = 205.6\,\mu$; $\sigma_{y,LER} = \sigma_{Y,HER} = 3.79\,\mu$; $(\omega_0\tau_d)^{-1} = 2.9210^{-5}$, and the values $\Lambda_1 = 1.988$, $\Lambda_2 = 1.782$ have been used for numerical calculations unless specified otherwise.

At low bunch currents all eigen-values are real. At a threshold current, one of the mode becomes linearly unstable, Fig.6.

The threshold current depends on the detuning from the closest resonance and the beam offset Δy. Fig. 7 and Fig. 8. show the maximum growth rate of radial modes for the resonance $n_0 = 1$, $l_0 = -2$ vs detuning $\Delta m = -0.1 + 0.01i$, $i, 1, ..., 8$, and offset Δy_0. The later is given in units of the vertical rms $\Delta y_0/\sigma_2 = 0.1 + 0.2(j-1)$, $j = 1, ..., 10$.

Fig. 9 shows the growth rate of all radial modes of the matrix $M(I,I')$ at the nominal bunch currents. The matrix was discretized on the mesh $i, j = 100 \times 100$. At this current, there is only one linearly unstable mode.

It is worth noting that the number of radial modes depends on the rank of the matrix M, i.e. on the discretization step ΔI, and does not have physical meaning. However, only few of the modes are real coherent modes while other can be considered as single-particle modes. The first can be defined as modes whose widths are larger than ΔI. Such modes have the lowest maximum magnitude of the normalized eigen vector $|V|^2$.

Fig. 10 gives an example of the mode structure, i.e. $|V|^2$ and $|V^T|^2$ of the most unstable mode. The eigen-vectors of the most linearly stable mode (the mode with

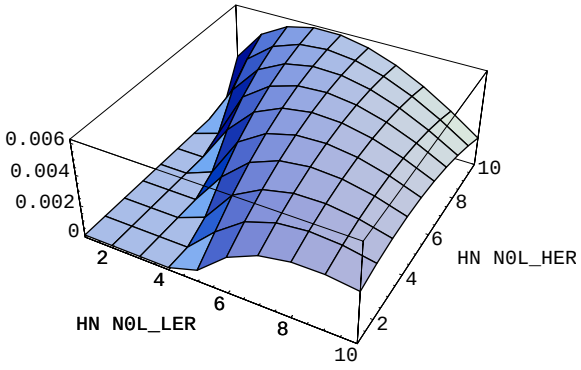

Figure 6: The fastest growth rate of the radial modes for the resonance $n = 2$, $l = -1$ vs beam currents. Bunch population $N/N0 = 1 + 0.2(i-1)$, $i = 1, ..., 10$; $Q_y\ LER = 34.64$; $Q_y\ HER = 23.64$

eigen-value which is complex conjugated to the eigen-value of the unstable mode) has the same structure. Nominal currents were used in calculations, $Qy_{HER} = 23.64$; $Qy_{LER} = 34.61$. The resonance $n_0 = 2$, $l_0 = -1$ detuned by $\Delta Q = -0.03$, was used as an example. Maximum linear growth rate in this case is for the mode 62, $\nu = 0.00479 + 0.0011\ i$, mode 61 is the most stable mode ($\mu = \nu^*$). The synchrotron radiation (SR) decrements were put to γ_0.

7 Interaction of Radial Modes.

Consider a resonance with azimuthal numbers n_0, l_0 neglecting all other azimuthal modes. At the threshold of instability, one of the radial modes V_ν becomes unstable. Time evolution of the mode depends on the interaction of this mode with linearly stable radial modes of the same resonance. This is true if the coherent tune shift of the radial modes is small compared to the distance to other linear resonances. How valid is this assumption depends on the choice of the working point in the tune diagram but usually appears naturally for the moderate beam-beam parameters.

It is convenient to describe mode interaction expanding azimuthal harmonics of the distribution function in radial eigen modes of the linear approximation,

$$\rho^{(1)}_{n0} = \frac{\partial \rho^{(1)}_H}{dI} e^{-in_0 Q_1 \phi + i\Delta m/2\phi} \sum_\mu A_\mu Y^\mu, \quad \rho^{(2)}_{n0} = \frac{\partial \rho^{(2)}_H}{dI} e^{-il_0 Q_2 \phi - i\Delta m/2\phi} \sum_\mu A_\mu X^\mu, \quad (30)$$

where X_μ and Y_μ are components of the vector $V_\mu = (X_\mu, Y_\mu)$ of the matrix M, Eq. (28), with the eigen-value μ. We assume that V_μ are normalized, $\int dI \hat{V}_\mu V_\nu = \delta_{\nu,\mu}$,

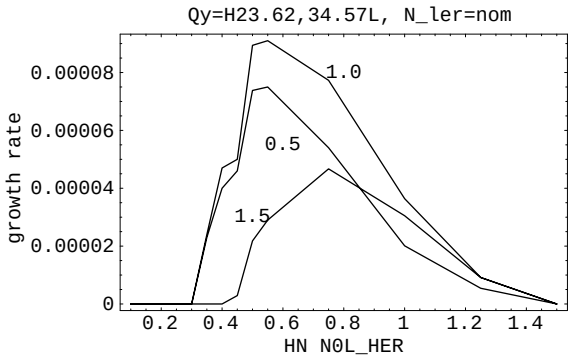

Figure 7: The maximum growth rate of radial modes for the resonance $n = 2$, $l = -3$. Q_y $LER = 34.57$, Q_y $HER = 23.62$, nominal bunch population. Beam offset is shown in units of σ_y.

where $\hat{V}_\mu$ is eigen-vectors of the transposed matrix M^T with the same eigen-value as vector V_μ.

Let us neglect all azimuthal modes $\rho_k(I,\phi)$ except modes in the resonance pair (n_0, l_0), and take into account only two radial modes: the linearly unstable mode V_ν and a linearly stable mode V_μ. The choice of V_μ will be specified later. We use notation for their amplitudes A_k, $k = 1$ for unstable mode ν, and $k = 2$ for stable mode with eigen-value μ. The amplitudes satisfy the system of two coupled equations

$$\frac{\partial A_k}{\partial \phi} + (i\lambda_k + \gamma_k)A_k = i\sum_{l=1}^{2} d_{k,l}A_l \tag{31}$$

where $\lambda_1 = \nu$, $\lambda_2 = \mu$, and synchrotron radiation (SR) decrement γ_k is given by

$$\gamma_k A_k = \int dI[\frac{\hat{X}_k R^{(2)}_{l0}}{[\rho^{(2)}_h]'}e^{i(l_0 Q_2 + \Delta m/2)\phi} + \frac{\hat{Y}_k R^{(1)}_{n0}}{[\rho^{(1)}_h]'}e^{i(n_0 Q_1 - \Delta m/2)\phi}], \tag{32}$$

where $R^{1,2}$ are given by Eq. (19). Here we used notation $[\rho]' = d\rho/dI$. The RHS is of the order of SR decrement γ_0 and small. This allows us to neglect mode coupling due to effect of the SR. In this case, Eqs. (32) define SR mode decrements. Fig.11 shows SR decrements calculated for the coherent radial modes which were defined as modes with width larger than $3\Delta I$. For other modes decrements were assumed to be equal to SR decrement γ_0. It is interesting to notice that the SR decrement for the unstable mode is minimal.

The coefficients $d_{k,l}$ describe mode coupling due to perturbation of the zero harmonics ρ_0 of the distribution function,

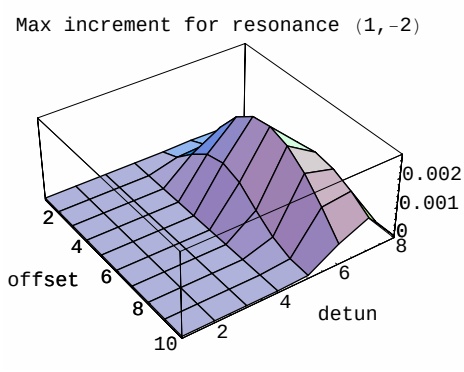

Figure 8: The maximum increment of radial modes for the resonance $n_0 = 1, l_0 = -2$ vs detuning $\Delta m/2$ and the offset Δy_0.

$$d_{k,l} = \int dI \hat{X}_k(I)\{(-\lambda_l + l_0\Delta Q_2 - \frac{\Delta m}{2})X_l\frac{[\rho_0^{(2)}]'}{[\rho_H^{(2)}]'} - 2\pi\Lambda_2 l_0 X_l \int dI \rho_0^{(1)}(I)\frac{dS_{00}(I,I)}{dI}\} \tag{33}$$

$$+\int dI \hat{Y}_k(I)\{(-\lambda_l + n_0\Delta Q_1 + \frac{\Delta m}{2})Y_l\frac{[\rho^{(1)}]'}{[\rho_H^{(1)}]'} - 2\pi\Lambda_1 n_0 Y_l \int dI \rho_0^{(2)}(I)\frac{dS_{00}(I,I)}{dI}\}. \tag{34}$$

Time variation of these coefficients can be obtained from Eq. (22),

$$\frac{\partial d_{kl}}{\partial \phi} + \gamma_0 d_{kl} = i\sum_{k',l'} P^{k,l}_{k',l'}[A_{k'}]^{c.c.}A_{l'}, \tag{35}$$

where parameters $P^{kl}_{k'l'}$

$$P^{k,l}_{k'l'} = -\int dI \frac{d}{dI}[(-\lambda_l + l_0\Delta Q_2 - \frac{\Delta m}{2})\frac{\hat{X}_k(I)X_l}{[\rho_H^{(2)}]'}] \times \frac{d}{dI}[(\lambda^{c.c.}_{k'} - \lambda_{l'})X^{c.c.}_{k'}X_{l'}(\rho_H^{(2)})'] \tag{36}$$

$$-\int dI \frac{d}{dI}[(-\lambda_l + n_0\Delta Q_1 + \frac{\Delta m}{2})\frac{\hat{Y}_k(I)Y_l}{[\rho_H^{(1)}]'}] \times \frac{d}{dI}[(\lambda^{c.c.}_{k'} - \lambda_{l'})Y^{c.c.}_{k'}Y_{l'}(\rho_H^{(1)})']. \tag{37}$$

Terms containing S_{00} are not written here. Their contribution is small.

8 Single mode in the Non-linear Regime

Let us consider first a simple case of a single unstable mode. Dynamics of the unstable mode is defined by perturbation of the distribution function ρ_0 by the

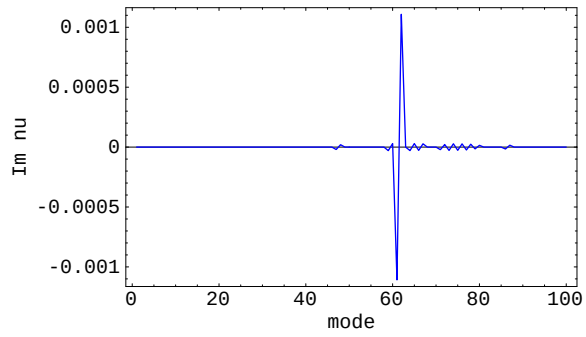

Figure 9: Linear growth rate of the radial modes. Nominal bunch population Nb. Resonance $n_0 = 2$, $l_0 = -1$

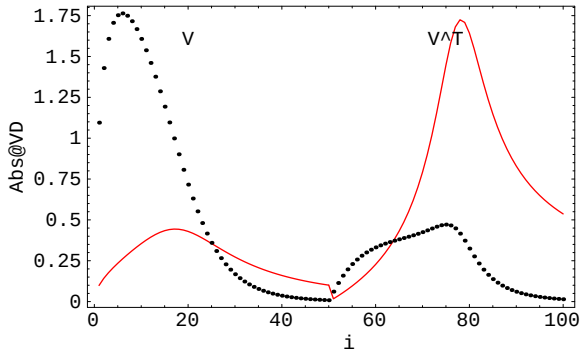

Figure 10: Eigen vectors V and V^T of the most unstable mode vs I/ϵ, $I/\epsilon = 0, ..., 5$. Left part of the curves $i = 1, ..., 50$ corresponds to vector X, right part to Y.

growing mode. This perturbation changes the growth rate and may lead to the mode saturation. This concept corresponds to the quasi-linear theory [4].

In this case, there is only one amplitude $A = A_1$, $d = d_{11}$, $P = P^{1,1}_{1,1}$, $\gamma = \gamma_1$ and the system Eqs. (31), (35) is reduced to

$$\frac{dA}{d\phi} + (i\nu + \gamma)A = idA, \quad \frac{\partial d(\phi)}{\partial \phi} + \gamma_0 d = iP|A|^2. \tag{38}$$

There is always a trivial solution $A = 0$ which gives the linear stability.

A nontrivial solution $\dot{d} = 0$, $d = d_0$, $A = A_0 e^{-i\Omega\phi}$, $Im[\Omega] = 0$ corresponds to unstable mode which saturates at some amplitude A_0 constant in time. The momentum d of ρ_0 is constant what corresponds to a steady-state beam distortion. Such a distortion may contribute to the well known flip-flop phenomena when at least one of the beams is blown-up. Eq. (38) defines amplitudes A_0, d_0 and the

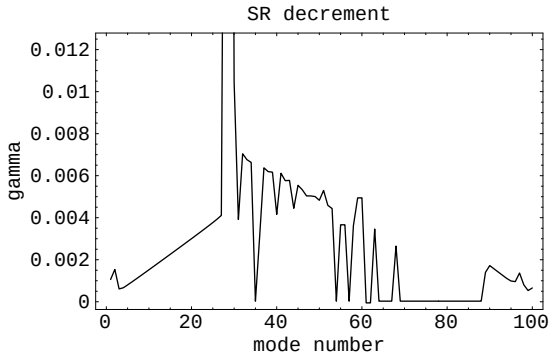

Figure 11: SR decrements of the radial modes. Nominal N_b, resonance $n_0 = 2$, $l_0 = -1$.

coherent frequency shift Ω,

$$|A_0|^2 = \gamma_0 \frac{(Im[\nu] - \gamma)}{Re[P]}, \quad d_0 = i\frac{P}{\gamma_0}A_0^2, \qquad \Omega = Re[\nu] + \frac{Im[P]}{Re[P]}(Im[\nu] - \gamma). \quad (39)$$

For a mode to be unstable, $Im[\nu] - \gamma$ has to be positive. Hence, solution Eq. (39) exists if $Re[P] > 0$. This condition is easy to meet because P is given by the second derivative of a function having maximum, see Eq. (36).

Condition of stability of the nontrivial solution can be obtained linearizing Eq. (38) $A = (A_0 + a)e^{-i\Omega\phi}$, $d = d_0 + c$:

$$\frac{da}{d\phi} + (i\nu + \gamma - i\Omega)a = i(d_0 a + A_0 c), \quad \frac{dc(\phi)}{d\phi} + \gamma_0 c = iPA_0(a + a^{c.c}). \quad (40)$$

By definition of the FP, cf. Eq. (38), $i\nu + \gamma - i\Omega = id_0$. Define phase ξ, $P = |P|e^{i\xi}$, and introduce g, b, and $c = ige^{i\xi}$, $a = be^{i\xi}$. Then,

$$\frac{dg}{d\phi} + \gamma_0 g = 2|A_0|Re[P]b, \quad \frac{db}{d\phi} + |A_0|g = 0. \quad (41)$$

The eigen-value $g, b \propto e^{i\zeta\phi}$ is

$$\zeta = \frac{i\gamma_0}{2} \pm \sqrt{2\gamma_0(Im[\nu] - \gamma) - (\frac{\gamma_0}{2})^2}. \quad (42)$$

Hence, the nontrivial solution is stable if $Im[\nu] > \gamma$, whereas the linear solution becomes unstable. Fig. 13 shows amplitude A vs. time for three initial values near the FP Eq. (39).

Harmonics $\rho^{(1)}_{n0}$ and $\rho^{(2)}_{l0}$ of the beam distribution oscillate and produce coherent signals at the frequencies $\omega_1 = n_0 Q_{1y} - \Delta m_0/2 + \Omega$ and $\omega_2 = l_0 Q_{2y} + \Delta m_0/2 - \Omega$, correspondingly.

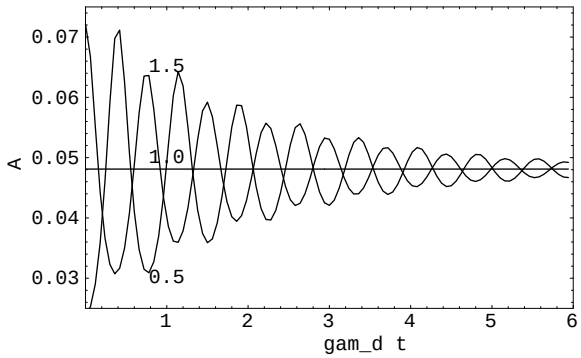

Figure 12: Beam dynamics in the vicinity of the single mode fix point (FP). Resonance $n_0 = 1$, $l_0 = -2$, linear growth rate $Im[\nu] = 0.0025$, SR damping rate $\gamma_d = 2.9210^{-5}$. Initial condition $d = d_0$ is given by Eq. (39). Three curves corresponds to initial amplitudes $A = A_0$, $A = 1.5A_0$, and $A = 0.5A_0$.

Non-trivial solution changes transverse beam emittance by $\Delta I = \int IdId\alpha\rho_0(I,\alpha)$. ΔI can be found from Eq. (22) where we approximate the RHS $R_0 \simeq -\gamma_0\rho_0$. This gives for the first beam

$$\frac{\partial}{\partial\phi}\Delta I_1 + \gamma_0\Delta I_1 = -2Im[\nu]|A_\nu|^2\int dId\alpha\frac{\partial\rho_H^{(1)}}{\partial I}|Y_\nu|^2, \tag{43}$$

where $\rho_H = \frac{1}{2\pi\epsilon}e^{-I/\epsilon}$. The blow-up in the steady-state is proportional to the increment $Im[\nu] > 0$ of the unstable mode

$$\Delta I_1 = \frac{2Im[\nu]}{\gamma_0\epsilon_1^2}|A_0|^2\int dIe^{-I/\epsilon}|Y_\nu|^2. \tag{44}$$

Here, A_0 is defined in Eq. (39) and, hence ΔI_1 is independent of γ_0. Result of the emittance variation is shown in Fig. 13.

Result for the second beam can be obtained by interchanging indexes $(1,2)$ and replacing Y_ν by X_ν.

In this section we have neglected of the coupling of the unstable mode to other radial modes. In the next section we show that such an interaction can lead to excitation of the linearly stable modes and periodic oscillations of the amplitudes.

9 Two Radial Modes

Next we consider two interacting modes where only one of them is linearly unstable with the eigen-value ν, $Im[\nu] > 0$. Initially, dynamics of the system is dominated by the exponentially growing mode A_ν. Eq. (35) shows that d_{ik} is driven by the term

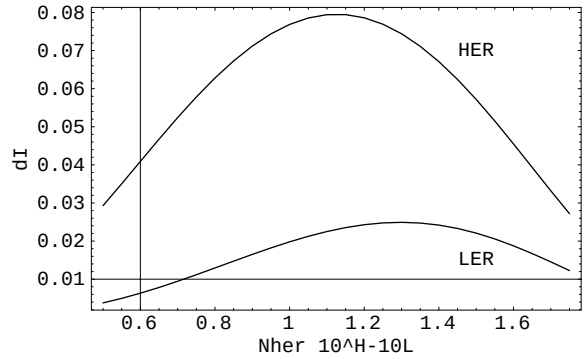

Figure 13: Variation of the vertical rms of the bunch $\Delta I/\epsilon_y$. $Qy_{LER} = 34.61$, $Qy_{HER} = 23.68$, sum resonance $n_0 = 2$, $l_0 = -1$. SR decrement $\gamma_0 = 2.9e-5$, linear $\nu = 0.0047 + 0.0011i$.

$\dot{d}_{i,k} = iP^{ik}_{\nu,\nu}|A_\nu|^2$. Let us neglect amplitudes of linearly stable modes and consider d_{ik} as constant. Then amplitude A_ν of the unstable mode grows in time with dynamic increment $\Gamma_\nu = Im[\nu] - \gamma_\nu - Im[d_{\nu\nu}]$. If $Re[P^{\nu,\nu}_{\nu,\nu}] > 0$, the dynamic increment goes at certain time to zero. The amplitude A_ν saturates at

$$|A^{sat}_\nu|^2 = \gamma_0 \frac{Im[\nu] - \gamma_\nu)}{Re[P^{\nu\nu}_{\nu\nu}]}. \tag{45}$$

From the equation for a linearly stable mode A_μ, $\mu \neq \nu$, follows in the same way that A_μ varies in time with the dynamic increment $\Gamma_\mu = Im[\mu] - \gamma_\mu - Im[d_{\mu,\mu}]$. At saturation, $d_{\mu,\mu} = (i/\gamma_0)P^{\mu,\mu}_{\nu,\nu}|A^{sat}_\nu|^2$ and

$$\Gamma^{sat}_\mu = Im[\mu] - \gamma_\mu - (Im[\nu] - \gamma_\nu)\frac{Re[P^{\mu\mu}_{\nu\nu}]}{Re[P^{\nu\nu}_{\nu\nu}]}. \tag{46}$$

If $\Gamma^{sat}_\mu > 0$, the linearly stable mode μ becomes unstable while linearly unstable mode ν saturates. This allows us to choose the most important stable mode as a mode with maximum positive Γ^{sat}_μ. Such a mode becomes unstable first and the amplitude A_μ may start to grow when the linearly unstable mode goes to saturation. Fig. 14 shows dynamic increments Γ^{sat}_μ for all radial modes. For the parameters used in calculations, the mode number 62 is linearly unstable while mode number 61 is the most linearly stable. At saturation, dynamic increment of the mode 62 goes to zero while dynamic increment of the mode 61 is slightly positive.

The criterion formulated for selection of the linearly stable mode shows that such a mode is the most stable mode in the linear approximation. Indeed, for such a mode $P^{\mu\mu}_{\nu\nu} = -[P^{\nu\nu}_{\nu\nu}]^{c.c}$ and the ratio $Re[P^{\mu\mu}_{\nu\nu}]/Re[P^{\nu\nu}_{\nu\nu}]$ is negative and maximal.

In this case, analysis of the fix points (FP) of the system is simplified. To simplify the notations, we change $\nu \to 1$, $\mu \to 2$. If mode 2 is the most stable mode in the

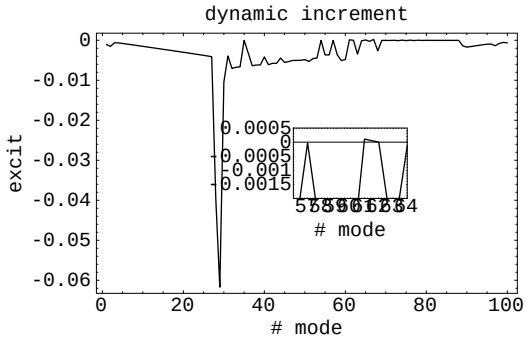

Figure 14: Dynamic increment of the radial modes. Nominal N_b, resonance $n_0 = 2$, $l_0 = -1$

linear approximation, then the eigen vectors V_1 and V_2 have the same pattern and coefficients P^{ik}_{lm} have symmetries:

$$P^{1,1}_{1,1} = -P^{1,1}_{2,2} = -[P^{2,2}_{1,1}]^{c.c} = [P^{2,2}_{2,2}]^{c.c}, \tag{47}$$

$$P^{1,2}_{1,1} = -P^{1,2}_{2,2} = -[P^{2,1}_{1,1}]^{c.c.} = [P^{2,1}_{2,2}]^{c.c}. \tag{48}$$

That leaves only two parameters $p = P^{1,1}_{1,1}/\gamma_0$, and $q = P^{1,2}_{1,1}/\gamma_0$. The FP solution $\partial d_{ik}/\partial\phi = 0$, $A_k \propto e^{-i\Omega\phi}$ with real Ω is given by

$$d_{1,1} = ipx, \quad d_{1,2} = iqx, \quad d_{2,1} = d^{c.c.}_{1,2}, \quad d_{2,2} = d^{c.c}_{1,1}, \tag{49}$$

$$|A_1|^2 = \frac{x|qx|^2}{|qx|^2 - (Im[\nu] - xRe[p] - \gamma)^2}, \quad \frac{A_2}{A_1} = \frac{Im[\nu] - xRe[p] - \gamma}{qx}. \tag{50}$$

The frequency shift $\Omega = Re[\nu] + xIm[p]$, and $x \equiv |A_1|^2 - |A_2|^2$ is defined by

$$x = \frac{1}{(Re[p])^2 - |q|^2}\{Im(\nu)Re[p] \pm \sqrt{(Im\nu)^2|q|^2 + \gamma^2[(Re[p])^2 - |q|^2}\}. \tag{51}$$

A solution exist if x is real. Stability of the solution can be analyzed linearizing Eqs. (31), (35).

Depending on parameters, interaction of two radial modes may lead to different beam behavior. If the amplitude at which a single linearly unstable mode saturates leaves the dynamic increment of linearly stable mode negative, the system goes to the single mode saturation regime described in the previous section. Otherwise, the linearly unstable mode excites the linearly stable mode before saturation and dynamics is defined by interaction of these two modes.

If in the system of two modes there are one or more fix points then, again, there are two possibilities. In the first, both modes go to saturation with some,

generally, non-equal amplitudes. Such a regime means that after transient period a new line appear in the spectrum while the line corresponding to initially unstable mode disappears. Another possibility is that the growing amplitude of linearly stable mode A_μ may change the dynamic increment of the mode A_ν and this mode starts to decay while, if $Re[P^{\mu\mu}_{\mu\mu}] > 0$, the amplitude A_μ saturates. The process can repeat itself and there will be periodic oscillations with energy exchange between modes. Such a mechanism is responsible for the onset of the saw-tooth instability [5].

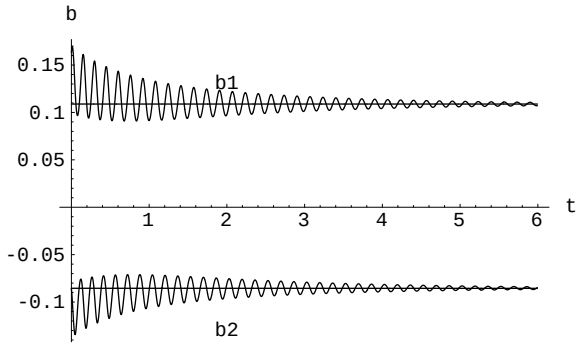

Figure 15: Oscillations in the system of two interacting radial modes with amplitudes b_1 and b_2. Time interval corresponds to 6 damping time. One mode (b_1) is linearly unstable, another one (b_2) is linearly most stable. Initial values for $b_1(0)$ is 0.5 of its value, $b_1 = 0.1088$, at FP. Other initial values are equal to their values at FP, in particular, $b_2(0) = -0.08547 + 0.0578\ i$. SR decrements of the modes are γ_0. Resonance $n_0 = 2$, $l_0 = -1$; detuning -0.03; nominal N_b

Beam dynamics in the system of two modes, the linearly unstable and the linearly most stable was considered for the resonance $n_0 = 2$, $l_0 = -1$ at nominal currents. Existence of the fixed points depends crucially on the SR decrements of the chosen modes. For SR decrements calculated by Eq. (32), no FP-s were found. The FP exists for SR decrements of both modes equal to γ_0. Time variation of the amplitudes of two modes $A = b\ e^{-i\Omega t}$ in this case was calculated by numerical integration of Eqs. (31) and (35) and is shown in Fig. 15. The total time interval corresponds to 6 damping time. Initial conditions corresponds to the FP for all parameters but $b_1(0)$ is 0.5 of b_1 at the FP.

10 Conclusion

The effect of the coherent beam-beam instability on the transverse emittance is considered for flat beams. Beam-beam coherent modes can be excited by periodic beam-beam kicks. Two types of resonances are considered. The first type, $Q_{1,2}(I) = m/n$, is due to resonance harmonics of the kicks produced by the opposite rigid

bunch in the steady-state. This type leads to resonances of non-linear oscillator under external periodic excitation. In the this case, rms emittance changes due to finite size of the separatrix of the resonance. Another type is due to sum resonances $nQ_1 - lQ_2 = m$; $n\dot{l} < 0$, in the system of two coupled beams. In this case, there are linearly unstable modes for bunch currents above threshold which saturate due to distortion of the bunch distribution by the unstable mode. The saturation may occur either for a single mode or due to interaction of unstable radial mode with linearly stable radial mode. Result depends crucially on the SR damping of the radial modes. Results are illustrated numerically. For the parameters of the PEP-II B-factory, saturation occurs already at a small fraction off the rms amplitudes. This is, probably, why coherent modes are so difficult to observe in experiments.

References

[1] See, for example,

A.W. Chao, Physics of High Energy Particle Accelerators, 1983, AIP Coference Proceedings, No. 1277, 1985 and references therein.

A. W. Chao, and R. Ruth Particle Accelerators, 16, 201, (1985)

K. Hirata The Beam-Beam Interaction:Coherent Effects, KEK Preprint 90-25, May 1990

K. Yokoya, Y. Funakoshi et al. Tune Shift of Coherent Beam-Beam Oscillations, Particle Accelerators V.27, p. 181, 1990

Y. Alexahin, Coherent Synchro-Betatron Oscillations in Colliding Beams, 14-th ICFA Beam Dynamics Workshop, Frascati, October 1997.

[2] PEP-II An Asymmetric B factory, CDR, June 1993, LBL-PUB-5379, SLAC-418, CALT-68-1869

[3] R.E. Meller, Ph.D. Thesis "Statistical Method for Nonequilibrium Systems with Application to Accelerator Dynamics", Cornell 1986

[4] Chin Chin Y., and Yokoya K., Nucl.Instr. and Methods, 1984, 226, 223-249.

[5] Heifets S.A., Non-linear Mode Coupling and Saw-Tooth Instability, Workshop on Instabilities in HHigh Intensity Hadron Beams in Rings, Brookhaven, June 1999.

11 Appendix 1. Basic Kinematics

A particle is located at $s_b = \pm ct - z - s_c$ at the moment t where z is position of a particle within a bunch, s_c is distance of a bunch from the head of the train.

The beam-beam vertical force to a particle in the first beam is defined by the Coulomb force F_y doubled to take into account effect of the magnetic field and averaged over the transverse distribution of the second bunch: $\int dxdy\rho = 1$. The force gives vertical kick $m\gamma c\Delta(dy/ds) = \int dtF_y^{(1)}$. Because transverse size of a bunch is much smaller than typical longitudinal distances, the kick can be written as

$$\Delta(dy_1/ds) = \frac{2N_b^{(2)}r_0}{\gamma_1}\int dx_2dy_2\rho_2(x_2,y_2)\frac{(y_2-y)}{[(x_1-x_2)^2+(y_1-y_2)^2]}. \tag{52}$$

We assume the factorized $\rho(x,y) = \rho(y)\rho_{\sigma_x}(x)$ with the Gaussian distribution in x-plane. Then

$$\Delta(dy_1/ds) = -\frac{2N_b^{(2)}r_0}{\gamma_1}\int dy'\rho_2(y')(y'-y_1)\int_0^\infty \frac{dt}{\sqrt{1+2t\Sigma_x^2}}e^{-t(y_1-y')^2}e^{-\frac{(x_1^0-x_2^0)^2t}{1+2\Sigma_x^2t}}, \tag{53}$$

where $\Sigma_x^2 = [\sigma_{1,x}]^2+[\sigma_{2,x}]^2$, all quantities are taken at the IP, and $x_{1,2} = D_{1,2}^{(x)}\delta_{1,2}\pm\Delta x$, $2\Delta x^0$ is horizontal beam separation, and $D^{(x)}$ is horizontal dispersion at IP.

The Hamiltonian for the first beam is

$$\hat{H}_1(y,q,s) = \frac{q^2}{2}+\frac{g(s)y^2}{2}+\delta(s)\int_0^y dy\Delta(dy/ds), \tag{54}$$

where $q = dy/ds$, and $g(s)$ is betatron focusing function. The last term here describes beam-beam interaction.

Introduce betatron phase

$$\phi = \frac{1}{Q_y}\int\frac{ds}{\beta(s)}, \quad \phi(s+2\pi R) = \phi(s)+2\pi, \tag{55}$$

where $\beta = w^2(s)$ is vertical beta-function, $w''+g(s)w = 1/w^3$, $\alpha = -wdw/ds$, and replace y,q by variables Y,P using generating function $\Pi(Y,q,s) = wqY+\alpha Y^2/2$. The variables are related: $y = \Delta y^0+wY$, and $q = (P-\alpha Y)/w$, where Δy^0 is vertical beam separation at IP.

The new Hamiltonian of the system is $H(Y,P,\phi) = \beta_yQ_y(\hat{H}-\partial\Pi/\partial s)$,

$$H(Y,P,Y',P',\phi) = H_1(Y,P,\phi)+H_2(Y',P',\phi), \tag{56}$$

$$H_1(Y,P,\phi) = \frac{Q_{1,y}P^2}{2}+\frac{Q_{1,y}Y^2}{2}+\Lambda_1V_1, \quad \Lambda_1 = \frac{2N_b^{(2)}r_0}{2\pi\gamma_1}, \tag{57}$$

where

$$V_1(Y,P,\phi) = 2\pi\delta(\phi)\int dY'dP'\rho_2(Y',P')S(\Delta y^0+w_1Y-w_2Y'), \tag{58}$$

$$S(y) = -\frac{1}{2}\int_0^\infty\frac{dt}{t\sqrt{1+t}}[e^{-\frac{t}{2}(\frac{y}{\Sigma})^2}-1]e^{-\frac{(x_1^0-x_2^0)^2}{\Sigma_x^2}\frac{t}{1+t}}. \tag{59}$$

Here $\Delta y^0 = \Delta y_1^0 - \Delta y_2^0$ is vertical beam separation which includes effect of the vertical dispersion, and $\delta(\phi)$ is periodic $\delta(\phi + 2\pi) = \delta(\phi)$.

Effect of the beam-beam interaction depends on the beam-beam parameter ξ^{BB}, $\Lambda V/\epsilon \simeq \xi_{BB}$,

$$\xi_1^{BB} = \frac{N_b^{(2)} r_0 \beta_{1,y}^*}{2\pi\gamma_1\sigma_{2,y}(\sigma_{2,x} + \sigma_{2y})}, \tag{60}$$

which is usually small, $\xi < 0.05$.

12 Appendix 2. The Steady-state Distribution

The steady-state can be described by the Hamiltonian averaged over ϕ. Then, below the threshold of coherent instability, action-angle variables I, α can be chosen to make Hamiltonian $H(I)$ independent of α.

Particle trajectory in this case can be expanded into even azimuthal harmonics

$$Y = \sqrt{2I}\cos\alpha + \Lambda_1 \sum_{k=0} a_k(I)\cos(k\alpha), \tag{61}$$

provided effect of damping and diffusion on trajectory is neglected and motion is reversible in time. Identity $Q_1 P = \{H, Y\}_{P,Y} = \omega(I)\partial Y/\partial\alpha$ defines

$P = -(\omega(I)/Q_1)[\sqrt{2I}\sin\alpha + \Lambda_1 \sum k a_k \sin(k\alpha)]$.

Expand $S(I, I', \alpha, \alpha', \Delta y_0) = S[\Delta y^0 + w_1\sqrt{2I}\cos\alpha - w_2\sqrt{2I}\cos\alpha]$, where Δy_0 is the vertical beam separation at IP, in azimuthal harmonics

$$S(I, I', \alpha, \alpha', \Delta y_0) = \sum_{n,l} S_{n,l}(I, I', \Delta y_0) e^{i(n\alpha - l\alpha')}, \tag{62}$$

For a flat beam, neglecting anharmonic corrections a_k to the trajectory and factor $e^{-(\Delta x)^2/2\Sigma_x^2}$,

$$S_{n,l}(I, I, \Delta y_0) = -\int_0^\infty \frac{d\xi}{\xi}\mathrm{Erfc}[\xi]\{\cos[(n-l)\frac{\pi}{2} + \frac{\Delta y_0\sqrt{2}}{\Sigma_x}\xi] J_n(\frac{2w_1\sqrt{I}}{\Sigma_x}\xi) J_l(\frac{2w_2\sqrt{I}}{\Sigma_x}\xi) - 1\}. \tag{63}$$

Here $\mathrm{Erfc}(\xi) = e^{\xi^2}[1 - \mathrm{Erf}(\xi)]$, $\mathrm{Erf}(\xi)$ is error function. For flat beam the main contribution is given by large $\xi >> 1$. In this case, $\mathrm{Erfc}(\xi) \simeq 1/(\xi\sqrt{\pi})$.

Anhramonic components in Eq. (61) give small terms of the order of $w\Lambda a_k/\Sigma_x$.

The steady-state distribution functions $\rho_H^{(1,2)}(I)$ of two beams, $2\pi \int dI \rho_H(I) = 1$, is approximately $\rho_H(I) = \frac{1}{2\pi\epsilon} e^{-I/\epsilon}$ where $\epsilon = \sigma^2/\beta$ is the transverse beam emittance.

The full distribution function $\rho(I, \alpha, \phi)$ is represented by the sum of azimuthal harmonics

$$\rho_1(I, \alpha, \phi) = \rho_H^{(1)}(I) + \sum_{n=-\infty}^{\infty} \rho_n^{(1)}(I, \phi) e^{in\alpha}, \quad \rho_{-n} = \rho_n^{c.c.} \tag{64}$$

Expand distribution function potential V Eq.(58) in azimuthal harmonics

$$V_1(I,\alpha,\phi) = 2\pi\delta(\phi)\sum V_n^{(1)}(I,\phi)e^{in\alpha} \tag{65}$$

where

$$V_n^{(1)}(I,\phi) = \int dId\alpha[S_{n,0}(I,I,\Delta y_0)\rho_H^{(2)}(I) + \sum_{l=-\infty}^{\infty} S_{n,l}(I,I,\Delta y_0)\rho_l^{(2)}(I)]. \tag{66}$$

Then, the Hamiltonian in the angle-action variables is $H(I,\alpha,\phi) = H_1 + H_2$ where

$$H_1(I,\alpha,\phi) = \frac{Q_1}{2}(P^2+Y^2) + \Lambda_1\sum_{n,m} e^{in\alpha - im\phi}V_n^{(1)}(I,\phi). \tag{67}$$

By definition, in the steady-state, all $\rho_l = 0$ and Hamiltonian H_1 has to be averaged over ϕ. This gives $H_H = H_H^{(1)}(I) + H^{(2)}(I)$,

$$H_H^{(1)}(I) = \frac{Q_1}{2}(P^2+Y^2) + \Lambda_1\sum_n e^{in\alpha}\int dId\alpha S_{n,0}(I,I,\Delta y_0)\rho_H^{(2)}(I). \tag{68}$$

Integration in the second term can be carried out explicitly if $\rho(I) = (1/\epsilon)e^{-I/\epsilon}$:

$$\int dId\alpha S_{n,0}(I,I,\Delta y_0)\rho_H^{(2)}(I) = -\int_0^\infty \frac{d\xi}{\xi}\mathrm{Erf}[\xi]J_n(\frac{2w_1\sqrt{I}}{\Sigma_x}\xi)\cos[n\frac{\pi}{2}+\frac{\Delta y_0\sqrt{2}}{\Sigma_x}\xi]e^{-(\sigma_{2,y}\xi/\Sigma_x)^2}. \tag{69}$$

The action-angle variables can be chosen in such a way that non-zero azimuthal harmonics of the potential cancel the non-zero harmonics of the terms Y^2+P^2 of the linear part of the Hamiltonian Eq.(57). Then, for flat beams and in the first approximation in Λ,

$$H_H^{(1)}(I) = \frac{Q_1}{2}[I + \Lambda_1\sqrt{2I}a_1(I)][1+\frac{\omega^2}{Q_1^2}] \tag{70}$$

$$-\frac{\Lambda_1\sigma_{2y}}{\sqrt{\pi}\Sigma_x}\int_0^\infty \frac{dx}{x^2}J_0(\frac{2w_1\sqrt{I}}{\sigma_{2,y}}x)\cos[\frac{\Delta y_0\sqrt{2}}{\sigma_{2,y}}x]e^{-x^2}. \tag{71}$$

This defines frequency $\omega_1(I) = dH/dI$, $\omega_1(I) = Q_1 + \Delta Q_1$, where

$$\Delta Q_1(I) = \Lambda_1 Q_1\frac{\partial}{\partial I}[\sqrt{2I}a_1(I)] + \frac{\partial}{\partial I}[I\Delta\omega] + \frac{\Lambda_1 w_1}{\Sigma\sqrt{\pi I}}\int_0^\infty \frac{dx}{x}J_1(\frac{2w_1\sqrt{I}}{\sigma_2}x)\cos(\frac{\Delta y_0\sqrt{2}}{\sigma_2}x)e^{-x^2}. \tag{72}$$

Anharmonic corrections to the trajectory can be defined by requiring cancellation of the non-zero harmonics. With the help of the identity

$$\frac{\partial H}{\partial Y} = -\{H,P\} = -\omega(I)\frac{\partial P}{\partial\alpha} = \frac{\omega^2(I)}{Q_1}[\sqrt{2I}\cos\alpha + \Lambda_1\sum k^2 a_k\cos(k\alpha)], \tag{73}$$

Eq.(68) averaged over ϕ gives

$$\frac{\partial H}{\partial Y} = Q_1 Y + \Lambda_1 w_1 \frac{\partial}{\partial \Delta y^0} \sum V_n(I, \Delta y_0) e^{in\alpha}. \tag{74}$$

Eqs. (73) and (74) give for amplitudes $a_k(I)$:

$$Q_1[\sqrt{2I}\cos\alpha + \Lambda_1 \sum a_k \cos(k\alpha)] + \Lambda_1 w_1 \sum_k \frac{\partial V_k}{\partial \Delta y^0} e^{ik\alpha} = \frac{\omega^2(I)}{Q_1}[\sqrt{2I}\cos\alpha + \Lambda_1 \sum k^2 a_k \cos(k\alpha)]. \tag{75}$$

Here $\Lambda_1 V_k$ are given by the second term in Eq. (68).

The coefficients of the first harmonics define $\Delta\omega$

$$\Delta Q_1(I) = \frac{\Lambda_1 w_1}{\Sigma_x \sqrt{\pi I}} \int_0^\infty \frac{dx}{x} J_1(\frac{2w_1\sqrt{I}}{\sigma_{2y}} x) \cos(\frac{\Delta y_0 \sqrt{2}}{\sigma_{2y}} x) e^{-x^2}. \tag{76}$$

For small offsets $\Delta y_0 << \sigma_y$, $\Delta\omega$ is proportional to degenerate hyper-geometric function

$$\Delta Q_1(I) = \frac{\Lambda_1 \beta_1}{2\Sigma\sigma_2} F(\frac{1}{2}, 2, -(\frac{\sigma_1}{\sigma_2})^2 \frac{I}{\epsilon_1}]. \tag{77}$$

For small z, $F(\alpha, \gamma, -z) = 1 - (\alpha/\gamma)z$. Hence, for small I,

$$\Delta Q_1 = \xi_{BB}^{coh}[1 - (\frac{\sigma_{1,y}}{2\sigma_{2,y}})^2 \frac{I}{\epsilon_{1y}}]. \tag{78}$$

Here we use the beam-beam parameter Eq. (2) where $\sigma_{2x} + \sigma_{2y}$ is replaced by Σ_x, $\xi_{BB}^{coh} = \Lambda_1\beta_1/(2\Sigma_x\sigma_{2y})$. For a small I, Eq. (78) corresponds to Hamiltonian

$$H = (Q_1 + \xi_{BB}^{coh})I - \frac{\Lambda_1 \beta_1^2}{16\Sigma_x \sigma_{2y}^3} I^2. \tag{79}$$

At a large z,

$$F(\alpha, \gamma, -z) = 2^{2-\gamma} \frac{\Gamma(\gamma)}{\Gamma(\alpha)\Gamma(\gamma - \alpha)\ z}, \tag{80}$$

and ΔQ decreases as $1/I$.

Comparing this with Eq. (70), we get

$$\Lambda_1 a_1 = -\frac{\Delta\omega(I)}{Q_1}\sqrt{\frac{I}{2}}. \tag{81}$$

This modifies the first harmonics of Y to $Y = \sqrt{2I/(1 + \Delta\omega/Q_1)}\cos\alpha$.

All other amplitudes a_k, $k > 1$ are given by Eq. (75),

$$[Q_1^2 - k^2\omega^2]a_k(I) = \frac{2w_1 Q_1}{\Sigma}\sqrt{\frac{2}{\pi}} \int_0^\infty \frac{dx}{x} J_k(\frac{2w_1\sqrt{I}}{\sigma_2} x) \sin[k\frac{\pi}{2} + \frac{\Delta y_0\sqrt{2}}{\sigma_2} x] e^{-x^2}. \tag{82}$$

Relative anharmonic corrections to trajectory is of the order of $\Lambda_1 a_k/\sqrt{I}$ or, for $I \simeq \epsilon_y$, of the order of ξ_{BB}/Q_y.